Available online at www.sciencedirect.com
ScienceDirect
Bioorganic Chemistry 35 (2007) 243–257
BIOORGANIC CHEMISTRY
www.elsevier.com/locate/bioorg

Tacrine derivatives–acetylcholinesterase interaction: ^{1}H NMR relaxation study

Maurizio Delfini [a,*], Maria Enrica Di Cocco [a], Fabiana Piccioni [a], Fernando Porcelli [b], Anna Borioni [c], Andrea Rodomonte [c], Maria Rosaria Del Giudice [c]

[a] *Dipartimento di Chimica, Università degli Studi "La Sapienza", piazzale Aldo Moro, 5 – 00185 Roma, Italy*
[b] *Dipartimento di Scienze Ambientali, Università della Tuscia, largo dell'Università, Blocco D– 01100 Viterbo, Italy*
[c] *Dipartimento del Farmaco, Istituto Superiore di Sanità, viale Regina Elena, 299 – 00161 Roma, Italy*

Received 23 October 2006
Available online 15 February 2007

Abstract

Two acetylcholinesterase (AChE) inhibitors structurally related to Tacrine, 6-methoxytacrine (**1a**) and 9-heptylamino-6-methoxytacrine (**1b**), and their interaction with Electrophorus Electricus AChE were investigated.

The complete assignment of the ^{1}H and ^{13}C NMR spectra of **1a** and **1b** was performed by mono-dimensional and homo- and hetero-correlated two-dimensional NMR experiments. This study was undertaken to elucidate the interaction modes between AChE and **1a** and **1b** in solution, using NMR. The interaction between the two inhibitors and AChE was studied by the analysis of the motional parameters non-selective and selective spin–lattice relaxation times, thereby allowing the motional state of **1a** and **1b**, both free and bound with AChE, to be defined. The relaxation data pointed out the ligands molecular moiety most involved in the binding with AChE. The relevant ligand/enzyme interaction constants were also evaluated for both compounds and resulted to be 859 and 5412 M^{-1} for **1a** and**1b**, respectively.

* Corresponding author. Fax: +39 06 490631.
E-mail addresses: maurizio.delfini@uniroma1.it (M. Delfini), mariaenrica.dicocco@uniroma1.it (M.E. Di Cocco), f.piccioni@uniroma1.it (F. Piccioni), porcelli@unitus.it (F. Porcelli), anna.borioni@iss.it (A. Borioni), andrea.rodomonte@iss.it (A. Rodomonte), mariarosaria.delgiudice@iss.it (M.R. Del Giudice).

0045-2068/$ - see front matter © 2007 Elsevier Inc. All rights reserved.
doi:10.1016/j.bioorg.2007.01.001

Keywords: Acetylcholinesterase from Electrophorus Electricus; Tacrine derivatives; ^{1}H NMR relaxation, interaction

1. Introduction

Alzheimer disease (AD), the most common form of dementia in the elderly, accounts for 50–60% of all dementia cases in the over 65 population. It leads to a progressive impairment in memory and cognitive abilities, and eventually to death. The cerebral regions associated with the highest and more complex functions, i.e., the cortex and hippocampus, are the most affected by AD degeneration.

To date, the only weapons against AD have been symptomatic treatments mostly based on the cholinergic approach, in particular on the inhibition of the acetylcholinesterase (AChE) activity [1,2] and on psycopharmacological agents used for the treatment of psychiatric aspects of the disease [3]. Over the last decade, drugs acting as inhibitors of the AChE, such as Tacrine, Rivastigmine Galantamine [4,5] and Donepezil [6] and the *N*-methyl-D-aspartate receptor antagonist Memantine [7], have been used to moderate the effects of cerebral degeneration. The biological aim of AChE inhibitors is to prevent the binding or the hydrolysis of the neurotransmitter acetylcholine, thus improving neuronal transmission. The inhibitors are likely to act according to a competitive mechanism, either by occupying the catalytic site or covalently reacting with the catalytic serine. Otherwise, as in the case of small molecules such as propidium [8], they can have an inhibiting function by interacting with a peripheral binding site situated on the catalytic gorge entrance.

Besides the cholinergic strategy, different therapeutic approaches are being intensively studied to find novel pharmacological agents for AD. Insights into the molecular basis of the degeneration have addressed the search for small molecules or peptides interfering in the amyloid formation or aggregation [7], and the employment of anti-inflammatory drugs [9], metal chelators [10], and antioxidants [11,12].

Recently, the finding of new AChE inhibitors has become anew the central target in developing drugs for the treatment of AD, as the latest studies have reported that patients treated with cholinesterase inhibitors did not show the widespread cortical atrophic changes associated with AD, providing empirical evidence of neuro-protection by cholinesterase inhibitors [13]. Despite being far as yet from an optimal pharmacological profile, AChE inhibitors are at present the only drugs used for the clinical treatment of AD.

So, this class of compounds has been the object of a renewed research effort. The novelty, with respect to the first generation of AChE inhibitors, is that multi-potent inhibitors simultaneously exhibiting several pharmacological properties are now used for a clinically effective approach. Indeed, it has been demonstrated that the achievement of potent inhibitors of the AChE catalytic site may not represent a significant improvement, unless there is a concomitant inhibition of the peripheral anionic site (PAS), which is associated with the neurotoxic AD cascade through AChE-induced Aβ aggregation [11]. Thus, those ligands which are able to interact simultaneously both with active and peripheral sites may eventually bring several advantages over the known inhibitors.

In this view, hybrid compounds with different properties were synthesized to obtain multi-potent anti-AD drugs [14–17] and recently, ''chimeric'' compounds were obtained from the reaction of Tacrine with carbamate compounds [18].

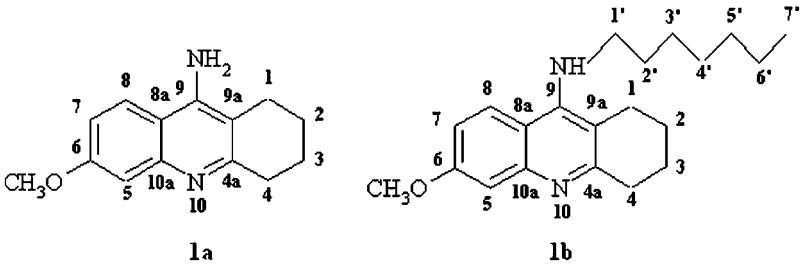

1a 1b

Fig. 1. Molecular structures of 6-methoxytacrine (**1a**) and 9-heptylamino-6-methoxytacrine (**1b**).

Potent Tacrine derivatives were synthesized by our group [19]. These derivatives showed an acute toxicity lower than Tacrine and a higher selectivity for AChE over BuChE, while Tacrine showed a relevant reverse selectivity profile. Consequently, these compounds seem to represent a good starting point for the synthesis of new multi-potent drugs.

The renewed interest in the development of novel Tacrine-based AChE inhibitors prompted us to undertake a study aimed at elucidating their mechanism of interaction with AChE in solution.

NMR is one of the most suitable techniques able to study ligand–macromolecules complexes and has been widely used for the study of the association equilibria in biological systems [20–22].

Nevertheless, only few studies concerning AChE-inhibitor interactions in solution are present [23–26], while several X-ray and molecular modelling applications have been carried out [27–33].

As a consequence, in this paper we have investigated the interaction of two Tacrine derivatives, 6-methoxytacrine (**1a**) and 9-heptylamino-6-methoxytacrine (**1b**), with acetylcholinesterase from Electrophorus Electricus (electric eel) by NMR spectroscopy (Fig. 1).

2. Materials and methods

The two Tacrine derivatives (**1a**,**1b**) were synthesized as previously reported [19]. AChE from Electrophorus Electricus (Tipe V-S from Sigma) was dialyzed, lyophilized, dissolved in phosphate saline buffer (PBS, pH 7.24) and used without further purification. Stock enzyme buffered solutions containing 1.7 mg/ml were prepared daily and AChE activity was evaluated by Ellman's method [34]. Stock enzyme buffered solution (0.25 ml) was added to 0.25 ml of inhibitors solutions at appropriate concentration. Ligand solutions were prepared in deuterium oxide-d_2 99.96% (Sigma) buffered at pH 7.24 (phosphate saline buffer) and carefully deoxygenated with a few freezing vacuum pumping thawing cycles immediately followed by sealing off the NMR tube.

NMR spectra of ligands were also performed in DMSO-d_6 (Sigma).

All NMR experiments were carried out on a Bruker Avance 400 spectrometer operating at 400.062 MHz for proton and at 100.577 MHz for ^{13}C.

Relaxation experiments were carried out on a 300 MHz Varian Mercury and 200 MHz Varian Gemini spectrometers operating at 299.99 MHz and 199.776 MHz for proton, respectively, at the controlled temperature of 300 ± 1 K. *Measurements conditions:* Varian

Mercury 300 MHz: 90° pulse length, 18 μs; 12 different τ values from 1 ms to 25 s; repetition rate, 25 s; Varian Gemini 200 MHz: 90° pulse length, 15 μs; 12 different τ values from 1 ms to 25 s; repetition rate, 25 s.

Chemical shifts were referenced to internal [d_4] 3-(trimethylsilyl) 3,3,2,2-tetradeuteropropionic acid Na salt (d_4-TSP).

2D-COSY spectra were obtained on Bruker Avance 400 spectrometer by using the pulse sequence available in the routine of the instrument at 300 K using 512 t1 increments with 2K data points and 32 scans each. Partial suppression of the residual HDO signal was accomplished by pre-saturation during the 1.5 s relaxation delay. The data were processed with a non-shifted sine-bell window in both dimensions. Spectral width was 8012 Hz in both dimensions.

HMQC experiment was performed using 512 t1 increments with 2K data points and 32 scans. Two zero-fillings were applied in the f1 dimension and a $\pi/3$ shifted squared sine-bell function was used in both dimensions.

Proton spin–lattice relaxation rates were measured with inversion recovery pulse sequences and calculated by exponential regression analysis of the recovery curves of longitudinal magnetization components.

Single- and double-selective proton spin–lattice relaxation rates were measured with inversion recovery pulse sequences implemented with DANTE or double-DANTE sequences [35,36]. All relaxation rates were calculated in the initial rate approximation [37].

3. Results and discussion

3.1. Peaks assignments

Up to date, most spectra of these compounds present in the literature have been carried out in organic solvents. For this reason, ^{1}H spectra were first performed in DMSO, and later on, in view of the ligand/enzyme study, spectra of the drugs were obtained in a phosphate buffer solution. As expected, the chemical shifts varied as the solvent varied, and they did also as a function of the concentration, with a consequent overlapping and some inversions of the signals, in particular of the aromatic protons.

That is likely to account for the chemical shift values we found, which are different from those of other works reported in the literature [38,39]. This behaviour was exhibited by both **1a** and **1b**.

Tables 1 and 2 report the ^{1}H chemical shifts of **1a** and **1b**, respectively, and their assignments. The latter were made on the basis of chemical shift values, comparison with model compounds, spectral multiplicities, and signal area values. The unequivocal assignments were performed by 2D NMR COSY experiments. As for the aromatic part of the two compounds, the correlation pattern is the same for both. Correlations between doublets at 7.21 ppm and 8.29 ppm (8.06 ppm for **1a**) allow the assignment of H-7 and H-8, respectively. The singlet at 7.10 ppm (7.01 ppm for **1a**) is assigned to H-5.

3.1.1. Alicyclic part

1a: Correlations between triplet at 2.52 ppm and multiplet at 1.91 ppm and between multiplet at 1.91 ppm and triplet at 2.91 ppm allow H-1 (2.52 ppm), H-2 (1.91 ppm), H-3 (1.91 ppm) and H-4 (2.91 ppm) to be unequivocally assigned.

Table 1
^{1}H chemical shifts and assignments of **1a** 0.3 mM in phosphate buffer (PBS 0.13 M, pH 7.24) and DMSO, $T = 300 \pm 1$ K

Position	δ (ppm) (PBS)	δ (ppm) (DMSO)
H-8	8.06	8.00
H-5	7.01	6.99
H-7	7.21	6.88
NH_2	—	6.19
MeO	3.96	3.80
H-4	2.91	2.76
H-1	2.52	2.48
H-2, H-3	1.91	1.77

Table 2
^{1}H chemical shifts and assignments of **1b** 0.3 mM in phosphate buffer (PBS 0.13 M, pH 7.24) and DMSO, $T = 300 \pm 1$ K

Position	δ (ppm) (PBS)	δ (ppm) (DMSO)
H-8	8.29	7.99
H-5	7.10	7.08
H-7	7.21	6.95
NH	—	5.25
MeO	3.98	3.82
H-1′	3.91	3.35
H-4	2.93	2.85
H-1	2.59	2.65
H-2, H-3	1.89	1.79
H-2′	1.77	1.52
H-3′	1.37	1.20
H-4′	1.28	1.20
H-5′, H-6′	1.23	1.20
H-7′	0.81	0.81

1b: Correlations between triplet at 2.59 ppm and multiplet at 1.89 ppm and between multiplet at 1.89 ppm and triplet at 2.93 ppm allow H-1 (2.59 ppm), H-2 (1.89 ppm), H-3 (1.89 ppm) and H-4 (2.93 ppm) to be unequivocally assigned. Moreover, correlations between triplet at 0.81 ppm and multiplet at 1.23 ppm, between multiplet at 1.23 ppm and multiplet at 1.28 ppm, between multiplet at 1.28 ppm and triplet at 1.37 ppm, between triplet at 1.37 ppm and triplet at 1.77 and between triplet at 1.77 and triplet at 3.91 ppm allow the assignments of H-7′ (0.81 ppm), H-6′, H-5′ (1.23 ppm), H-4′ (1.28 ppm), H-3′ (1.37 ppm), H-2′ (1.77 ppm) and H-1′ (3.91 ppm).

The structure was confirmed by ^{13}C NMR spectra performed in DMSO for each compound and in D_2O phosphate buffer. The unequivocal assignments of ^{13}C resonances were obtained by hetero-correlated ^{13}C–^{1}H 2D NMR experiments (HMQC).

The relevant chemical shifts are reported in Tables 3 and 4.

3.1.2. Aliphatic chain

The HMQC spectrum showed cross-peaks between H-1′/C-1′ (δ 3.91/49.2), H-2′/C-2′ (δ 1.77/31.4), H-3′/C-3′ (δ 1.37/28.0), H-4′/C-4′ (δ 1.28/29.9), H-5′/C-5′ (δ 1.23/32.9),

Table 3
^{13}C chemical shifts and assignments of **1a** 10 mM in PBS and DMSO

Position	δ (ppm) (PBS)	δ (ppm) (DMSO)
C-1	23.3	23.6
C-2	22.3	22.7
C-3	21.9	22.8
C-4	28.9	33.7
C-4a	156.0	157.7
C-5	99.5	114.6
C-6	163.9	159.1
C-7	118.7	106.7
C-8	125.1	123.3
C-8a	117.3	107.7
C-9	152.3	148.3
C-9a	110.2	111.9
C-10a	140.2	148.2
MeO	57.7	55.1

Table 4
^{13}C chemical shifts and assignments of **1b** 10 mM in PBS and DMSO

Position	δ (ppm) (PBS)	δ (ppm) (DMSO)
C-1	24.6	24.8
C-2	23.0	22.5
C-3	22.0	22.0
C-4	29.5	28.4
C-4a	157.1	158.0
C-5	99.8	106.8
C-6	163.9	159.2
C-7	117.6	115.5
C-8	127.9	124.5
C-8a	112.3	114.9
C-9	151.0	150.7
C-9a	110.8	114.0
C-10a	141.9	148.8
MeO	57.7	55.0
C-1′	49.2	48.1
C-2′	31.4	31.4
C-3′	28.0	26.2
C-4′	29.9	30.8
C-5′	32.9	33.6
C-6′	23.8	23.0
C-7′	15.2	14.0

H-6′/C-6′ (δ 1.23/23.8) and H-7′/C-7′ (δ 0.81/15.2). Consequently, we can assign C-2′ at 31.4 ppm, C-3′ at 28.0 ppm, C-4′ at 29.9 ppm, C-5′ at 32.9 ppm, C-6′ at 23.8 ppm and C-7′ at 15.2 ppm.

3.1.3. Aromatic ring

The following correlations are present: δ 8.29/127.9, δ 7.21/117.6, δ 7.10/99.8, allowing the assignments of C-8, C-7 and C-5, respectively.

3.1.4. Aliphatic ring

The following correlations were evidenced: δ 2.59/24.6 (H-1/C-1), δ 1.89/23.0 (H-2/C-2), δ 1.89/22.0 (H-3/C-3) and δ 2.93/29.5 (H-4/C-4).

The OCH_3 carbon signal was univocally assigned on the basis of the correlation between δ 3.98/57.7.

The long-range proton-carbon spectrum (optimized for two- and three-bond couplings) shows correlations between protons and carbons that are separated by two or three bonds. Correlations between the proton signal of H-8 at 8.29 ppm with the carbon signals at 141.9 ppm, 151.0 ppm and 163.9 ppm allow assignments of C-10a, C-9 and C-6, respectively, the latter one being confirmed by the correlation with MeO protons at 3.98 ppm. The proton signal of H-7 at 7.21 ppm correlates with the carbon signal at 112.3 ppm allowing the assignment of C-8a. Therefore, the C-9a at 110.8 ppm signal can be unequivocally assigned.

The carbon shifts of **1a** (Table 3) were assigned by the same one- and two-dimensional homo- and hetero-nuclear NMR techniques as used for **1b**.

3.2. Motional parameters

The investigation of **1a** and **1b** interactions with AChE in phosphate buffer was carried out by first considering the structural parameter chemical shift. Ligand solutions at different concentrations and ligand–AChE solutions at different molar ratios were studied.

Chemical shifts of **1a** and **1b** protons in the presence of AChE and at several ligand–AChE molar ratios showed very small differences.

Such a behaviour is expected in ligand–macromolecules diamagnetic complexes, where the effects on chemical shift are very small under fast exchange conditions, even in the presence of a high binding constant [40].

The macromolecule (~260 kD), although present in a very small quantity, can strongly affect the motional behaviour of the ligand [25,26]. Indeed the data obtained by NMR motional parameters, such as the spin–lattice relaxation rates ($R_i = 1/T_1$), give more information, with the relaxation mechanism for any proton H_i being mainly provided by the dipole–dipole interactions with protons nearby, such that

$$R_i^{NS} = \sum_{j \neq i} \rho_{ij} + \sum_{j \neq i} \sigma_{ij} + \rho_i^*$$

where $R_i^{NS} = 1/T_1^{NS}$ ρ_{ij} and σ_{ij} are the direct- and cross-relaxation rates relative to the H_i–H_j dipolar interaction, respectively, and ρ_i^* accounts for possible contributions from other relaxation mechanisms. Such a rate is labelled NS (non-selective) in order to emphasize that all proton resonances are excited by the same irradiation field, so that all spin populations are perturbed from their equilibrium values. Relaxation rates are related to the correlation time for molecular reorientation τ_c, an intrinsic motional parameter of any proton nucleus. The motional properties of molecular moieties can be properly described by the correlation times measured on the basis of the spin–lattice relaxation times (T_1^{NS}) ratio at different magnetic fields [41], using the equation

$$\frac{T_1^{NS}(\omega_1)}{T_1^{NS}(\omega_2)} = \frac{R_1^{NS}(\omega_2)}{R_1^{NS}(\omega_1)} = \frac{(5 + 8\omega_2^2\tau_c^2) \cdot (1 + 5\omega_1^2\tau_c^2 + 4\omega_1^4\tau_c^4)}{(5 + 8\omega_1^2\tau_c^2) \cdot (1 + 5\omega_2^2\tau_c^2 + 4\omega_2^4\tau_c^4)} \quad (1)$$

where ω_1 and ω_2 are the proton Larmor frequencies at certain magnetic fields. Hence, τ_c for any proton can be evaluated when knowing the T_1^{NS} values at two different frequencies.

The experimental spin–lattice relaxation ratios and τ_c values as evaluated using Eq. (1) for **1a** and **1b** alone and in interaction with AChE (AChE:ligand ratio 1:100), both in phosphate buffer, are reported in Tables 5 and 6.

Data indicate that in the presence of AChE both compounds show a more marked rotational slowing down of the aromatic moiety with respect to the alicyclic portion, and for compound **1b** also with respect to the aliphatic chain. In the aliphatic chain of **1b** a significant slowing down of the rotational motion is only exhibited by CH_3 in position 7′. Such a behaviour may be ascribed to hydrophobic interactions with aromatic amino-acids covering the gorge, analogously with other compounds [16]. The comparison between the τ_c values of the nuclei of the methoxy-heptyl derivative, the methoxy derivative and the Tacrine previously studied [42], seems to indicate a quite different AChE effect on compound **1b** than on Tacrine and compound **1a** (Fig. 2). $\Delta\tau_c$ for CH_3 (7′) is quite large and indicative of a strong re-orientational slowing down. The value is comparable with

Table 5
1a protons correlation times (τ_c) in absence (*a*) and in presence (*p*) of AChE (AChE:**1a** ratio 1:100), measured on the basis of the equation in the text (concentration of **1a** = 0.3 mM)

Position	$\frac{T_1^{NS}(\omega_1)}{T_1^{NS}(\omega_2)}$ (*a*)	τ_c(*a*) (s)	$\frac{T_1^{NS}(\omega_1)}{T_1^{NS}(\omega_2)}$ (*p*)	τ_c (*p*) (s)
H-8	1.33	18.9×10^{-11}	1.58	31.4×10^{-11}
H-7	1.44	22.7×10^{-11}	1.51	27.2×10^{-11}
H-5	1.30	17.6×10^{-11}	1.56	29.7×10^{-11}
H-4	1.12	10.6×10^{-11}	1.22	14.7×10^{-11}
H-1	1.37	20.6×10^{-11}	1.42	22.4×10^{-11}
H-2/H-3	1.00	1.0×10^{-11}	1.04	6.8×10^{-11}
MeO	1.05	6.9×10^{-11}	1.14	11.7×10^{-11}

Errors on τ_c values are less than 0.2×10^{-11} (s).

Table 6
1b protons correlation times (τ_c) in absence (*a*) and in presence (*p*) of AChE (AChE:**1b** ratio 1:100), measured on the basis of the equation in the text (concentration of **1b** = 0.3 mM)

Position	$\frac{T_1^{NS}(\omega_1)}{T_1^{NS}(\omega_2)}$ (*a*)	τ_c (*a*) (s)	$\frac{T_1^{NS}(\omega_1)}{T_1^{NS}(\omega_2)}$ (*p*)	τ_c (*p*) (s)
H-8	1.31	18.2×10^{-11}	1.61	32.8×10^{-11}
H-7	1.41	22.3×10^{-11}	1.58	31.4×10^{-11}
H-5	1.28	17.1×10^{-11}	1.49	26.1×10^{-11}
H-4	1.14	11.7×10^{-11}	1.24	15.7×10^{-11}
H-1	1.37	20.6×10^{-11}	1.44	22.7×10^{-11}
H-2/H-3	1.08	8.6×10^{-11}	1.09	9.4×10^{-11}
MeO	1.04	6.8×10^{-11}	1.15	11.8×10^{-11}
H-1′	1.19	13.7×10^{-11}	1.23	15.6×10^{-11}
H-2′	1.14	11.7×10^{-11}	1.19	13.7×10^{-11}
H-3′	1.12	10.6×10^{-11}	1.15	11.8×10^{-11}
H-4′	1.09	9.4×10^{-11}	1.13	11.6×10^{-11}
H-5′/H-6′	1.09	9.4×10^{-11}	1.20	13.8×10^{-11}
H-7′	1.09	9.4×10^{-11}	1.34	19.8×10^{-11}

Errors on τ_c values are less than 0.2×10^{-11} (s).

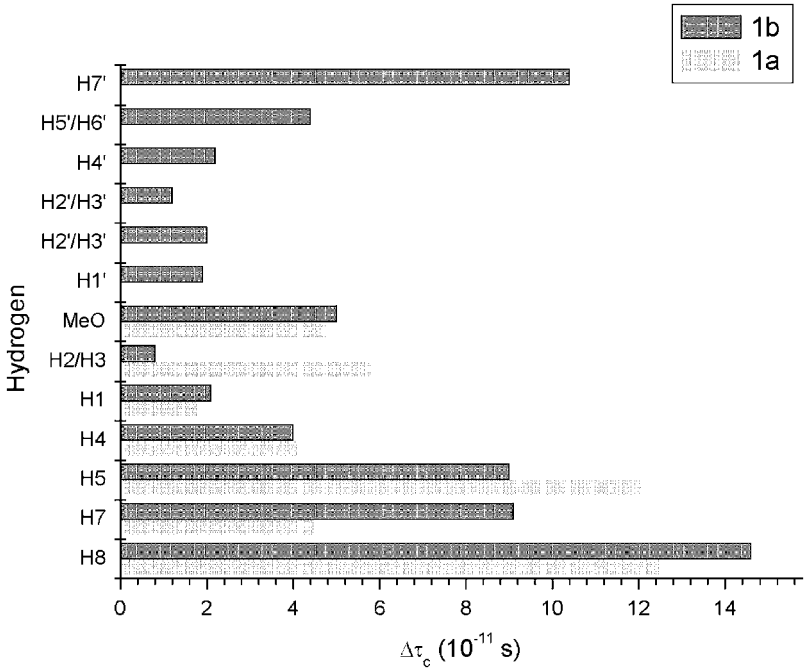

Fig. 2. Changes in the correlation times for each hydrogen of **1a** and **1b**.

$\Delta\tau_c$s for 7, 8 nuclei, the most involved in the interaction. Moreover, a chain length of 6 or 7 CH_2 groups seems to allow a good interaction with PAS AChE [26,43].

The motional correlation time can be also evaluated on the basis of the selective relaxation rates.

It is also possible to excite only one proton resonance, while leaving the rest of the spin system at equilibrium. It has been shown [35] that the spin–lattice relaxation rate measured in these conditions is given by the equation

$$R_i^{\mathrm{Sel}} = \sum_{i \neq j} \rho_{ij} + \rho_i^*$$

where Sel label means *selective*. As stated above, upon addition of AChE up to a protein:ligand ratio = 0.05, all chemical shifts were almost unaffected. Even in the presence of the protein at low molar ratios, **1a** and **1b** are expected to fast exchange between the free and the bound environments. Such exchange has been shown to yield a certain enhancement of selective proton spin–lattice relaxation rates, $R^{\mathrm{Sel}}(1/T_1^{\mathrm{Sel}})$ being much more affected than R^{NS}, as expected [35,40]. Selective relaxation times of **1a** and **1b** protons measured in the absence and presence of AChE are reported in Table 7. The obtained values confirm that protons of the aromatic moiety are the more affected by the interaction.

R_1^{ij} (s^{-1}) is the double-selective relaxation rate measured for H_i upon selective excitation of H_i and H_j:

Table 7
Selective relaxation times of **1a** and **1b** protons measured in the absence and presence of AChE

Proton	**1a** selective T_1 (s)	**1a** + AChE selective T_1 (s)	**1b** selective T_1 (s)	**1b** + AChE selective T_1 (s)
H-8	2.648	1.104	0.672	0.088
H-7	2.348	1.995	2.747	1.266
H-5	2.023	1.751	1.279	0.822
H-4	0.745	0.677	0.708	0.643
H-2,H-3	0.697	0.650	0.369	0.351
H-1	0.727	0.657	0.807	0.726
MeO	0.850	0.580	0.799	0.679
H-7′	—	—	2.132	1.445

Errors on the relaxation times are less than 3%.

$$R_1^{ij} = \sigma_{ij} + \sum_{i \neq j} \rho_{ij} + \rho_i^*$$

The correlation time is related to the dipolar interaction energy between protons at fixed distances, σ^{ij}, as measured by double-selective relaxation rates according to the equation [40]

$$\sigma^{ij} = R_1^{ij} - R_i^{\mathrm{Sel}} = \frac{1}{10}\frac{\gamma^4\hbar^2}{r_{ij}^6}\left\{\frac{6\tau_c^{ij}}{1+\omega^2(\tau_c^{ij})^2} - \tau_c^{ij}\right\} \tag{2}$$

where R_1^{ij} (s^{-1}) is the double-selective relaxation rate measured for H_i upon selective excitation of H_i and H_j, R_i^{Sel} is the selective relaxation rate measured for H_i, γ is the proton magnetogyric ratio (=26,753 $rads^{-1}\,G^{-1}$), ω is the proton Larmor frequency, $\hbar$ is the reduced Planck's constant ($\equiv h/2\pi = 1.0545887 \times 10^{-27}$ erg s rad^{-1}), r_{ij} is the H_i–H_j vector, and τ_c^{ij} is the motional correlation time characterizing reorientation of the H_i–H_j vector.

The cross-relaxation rates measured in the absence and in the presence of AChE ([ligand] = 0.3 mM; AChE:ligand ratio = 1:100), provide a means of improving the characterization of the binding interaction.

In the fast exchange conditions the equation

$$\sigma_{\mathrm{obs}}^{ij} = p_{\mathrm{free}}\sigma_{\mathrm{free}}^{ij} + p_{\mathrm{bound}}\sigma_{\mathrm{bound}}^{ij}$$

made it possible to evaluate σ^{ij} in the bound state ($\sigma_{\mathrm{bound}}^{ij}$).

The p fractions of the ligand in each environment can be approximated by $p_{\mathrm{bound}} = [\mathrm{protein}]/[\mathrm{ligand}]$, $p_{\mathrm{free}} = 1 - p_{\mathrm{bound}} \approx 1$. It follows that

$$\sigma_{\mathrm{obs}}^{ij} - \sigma_{\mathrm{free}}^{ij} = \Delta\sigma^{ij} = p_{\mathrm{bound}}\sigma_{\mathrm{bound}}^{ij}$$

The cross-relaxation rate in **1a** and **1b** becomes negative

$$\mathbf{1a}: \sigma_{\mathrm{free}}^{7,8} = \sigma_{\mathrm{free}}^{8,7} = 0.014s^{-1}; \sigma_{\mathrm{obs}}^{7,8} = \sigma_{\mathrm{obs}}^{8,7} = -0.052\ \mathrm{s}^{-1}$$

$$\mathbf{1b}: \sigma_{\mathrm{free}}^{7,8} = \sigma_{\mathrm{free}}^{8,7} = 0.028s^{-1}; \sigma_{\mathrm{obs}}^{7,8} = \sigma_{\mathrm{obs}}^{8,7} = -0.305\ \mathrm{s}^{-1}$$

thus indicating that the molecular motion is quite different in the absence and presence of AChE. The negative value of $\sigma_{\mathrm{obs}}^{7,8}$ suggests a lower mobility of the H-7 H-8 fragment. The $\sigma_{\mathrm{obs}}^{7,8}$ becomes negative as a consequence of the binding, thereby indicating that the corresponding inter-nuclear vector is modulated by relatively slow reorientation motions.

Among the obtained values, those for proton pairs of the aliphatic cycle cannot be easily interpreted because the σ^{ij} is contributed by the geminal interaction and by the vicinal interactions. Even for CH_3 (7′) protons, the σ values cannot be easily interpreted since they are affected by vicinal interactions. Consequently, the combined data of τ_c obtained by T_1 at two-fields ratio and σ demonstrate that fragment C7–H C8–H is the molecular moiety most involved in the binding with AChE.

Therefore, the $\sigma^{ij}_{\text{bound}}$ calculated for the H7–H8 proton pair can be further handled for evaluating the motional correlation time of the two inhibitors in the binding pocket by considering $r_{7,8} = 0.243$ nm.

Calculations (see Eq. (2)) provide, at $T = 300$ K, $\tau_{7,8} = 24$ ns for **1a** and $\tau_{7,8} = 120$ ns for **1b**, thus indicating that both inhibitors are differently bound to the protein. The nature of the fragment involved in the interaction suggests that it is an interaction of the π−π type between the ligand aromatic part and the aromatic amino acids covering the gorge, in agreement with what observed for Tacrine both via X-rays [27] and through molecular modelling and docking [31]. In our compounds, interaction involves mainly the C7–H C8–H fragment.

The definition of the molecular residue more involved in binding and the characterization of its motional parameters can be used for the evaluation of the corresponding binding constant.

Since

$$R^{\text{Sel}}_{\text{obs}} = p_{\text{free}} R^{\text{Sel}}_{\text{free}} + p_{\text{bound}} R^{\text{bound}}_{sel}$$

and $p_{\text{free}} = 1 - p_{\text{bound}} \approx 1$ it follows that

$$R^{\text{Sel}}_{\text{obs}} - R^{\text{Sel}}_{\text{free}} = \Delta R^{\text{Sel}} = p_{\text{bound}} R^{\text{Sel}}_{\text{bound}}$$

As already noticed elsewhere [35,40,44], the fact that ΔR^{Sel} is titratable by the ligand concentration at a fixed value of protein concentration demonstrates that the observed phenomena arise from binding to the protein with a consequent slowing down of molecular motions and are independent of viscosity. The occurrence of dipole–dipole interactions with protein protons is expected to contribute the relaxation rate enhancement. In the limit of 1:1 interaction at low [protein]/[ligand] ratios the following equation can be obtained [45]

$$\frac{1}{\Delta R^{\text{Sel}}_i} = \left\{ \frac{1}{K_{\text{int}}} + [L] \right\} \frac{1}{R^{\text{Sel}}_{i\text{b}} P_0}$$

where $[L]$ is the ligand concentration, P_0 is the total concentration of the protein and $R^{\text{Sel}}_{i\text{b}}$ is the selective rate in the bound environment. Titration of ΔR^{Sel} for affected protons allows evaluating the apparent dissociation constant by extrapolating data to $1/\Delta R^{\text{Sel}} = 0$ where $[L] = -K_{\text{int}}$. As a consequence, a plot of $1/\Delta R^{\text{Sel}}_i$ *vs.* the ligand concentration extrapolates at zero at $[L] = 1/K_{\text{int}}$. Selective spin–lattice relaxation times (T_1) of **1a** and **1b** H-8 in the absence and presence of AChE are reported in Tables 8 and 9, respectively, allowing the calculation of K_{int} (Figs. 3 and 4).

The calculated values ($K_{\text{int}} = 859\ \text{M}^{-1} \pm 18$ for **1a** and $K_{\text{int}} = 5412 \pm 27\ \text{M}^{-1}$ for **1b**) suggest that the two inhibitors are differently bound by AChE, **1b** being much more tightly bound than **1a**.

As a consequence, the larger the ΔR^{Sel}, the faster the corresponding selective relaxation rate in the bound state. Such a rate is determined by reduced molecular motions

Table 8
Selective spin–lattice relaxation times (T_1) of **1a** H-8 in the absence and presence of AChE

1a concentration (mM)	**1a** selective T_1 (s)	**1a** + AChE selective T_1 (s)	ΔR (s^{-1})	$1/\Delta R$ (s)
0.2	2.620	1.045	0.575	1.739
0.3	2.648	1.104	0.528	1.894
0.4	2.748	1.156	0.501	1.996
0.5	2.686	1.189	0.469	2.132

Errors on the relaxation times are less than 3%.

Table 9
Selective spin–lattice relaxation times (T_1) of **1b** H-8 in the absence and presence of AChE

1b concentration (mM)	**1b** selective T_1 (s)	**1b** + AChE selective T_1 (s)	ΔR (s^{-1})	$1/\Delta R$ (s)
0.3	0.672	0.088	9.901	0.101
0.6	0.672	0.128	6.329	0.158
0.7	0.663	0.145	5.376	0.186
0.8	0.675	0.156	4.926	0.203

Errors on the relaxation times are less than 3%.

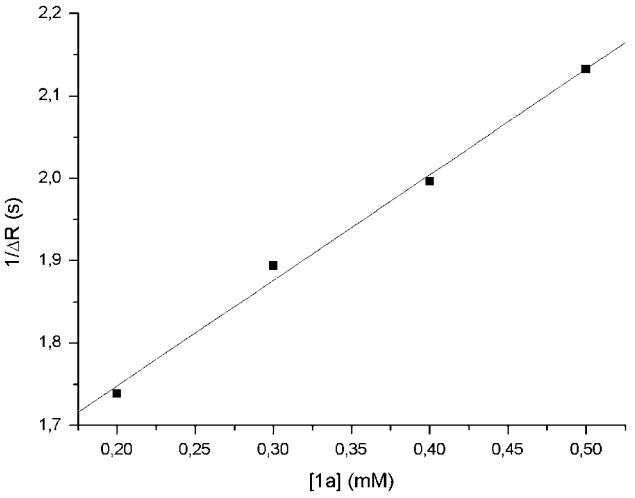

Fig. 3. Behaviour of $1/\Delta R_{Sel}$ of **1a** H-8 proton as a function of concentration. The AChE concentration is 3 μM.

accompanied by dipole– dipole interactions with protein protons. To note that the nuclei of aromatic moieties of **1a** and **1b** are the most affected in both molecules, indicating a different binding energy.

Different interaction constants are obtained. The heptyl derivative shows a constant higher than the *N*-unsubstituted methoxy derivative and confirms data concerning compounds substituted on 9-amino groups, which resulted stronger AChE inhibitors than the corresponding unsubstituted ones [43]. The NMR data appear to be in good agreement with the pharmacological data IC_{50}. In fact **1b** shows an IC_{50} value almost comparable with Tacrine and lower than *N*-unsubstituted methoxy.

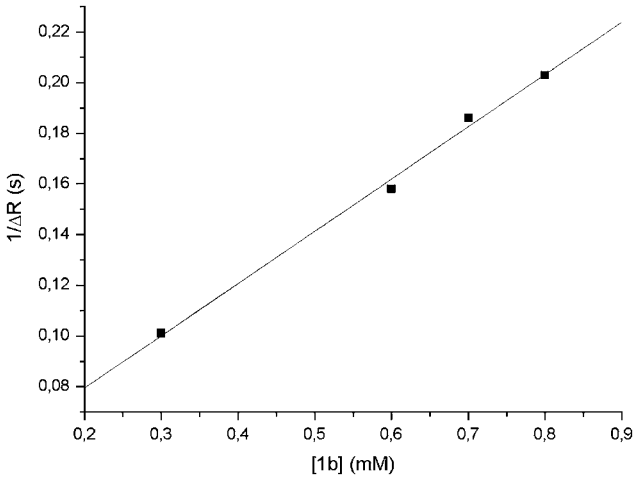

Fig. 4. Behaviour of $1/\Delta R_{Sel}$ of **1b** H-8 proton as a function of concentration. The AChE concentration is 3 μM.

In recent Tacrine–AChE interaction studies, the IC_{50} values have been related to binding free energy ΔG_{bind} [46,47] and to inhibition free energy $\Delta G_{inh,}$ the latter representing the absolute free energy of inhibition in protein solvent environment. A good correlation has been evidenced according to which lower values of ΔG_{bind} correspond to lower values of IC_{50}. The interaction constant values obtained by NMR data confirm this trend. Actually, **1a** exhibits a lower constant and a higher IC_{50} than **1b**. Furthermore, the two inhibitors show a different kinetic behaviour. The kinetic constant values for Tacrine and **1a** indicate a mixed competitive–uncompetitive inhibition mechanism [34]. On the contrary, **1b** shows a significant different inhibitory pattern with respect to Tacrine, with similar inhibition constant but a ($1/K_{UNC}$) much lower value, specific of a competitive inhibition pattern.

6-Methoxytacrine showed an affinity for AChE comparable to that of Tacrine and exhibited an identical inhibitory pattern. In fact, the introduction of the methoxy group in position 6 of the aminoacridine ring, which is functional to increase the electron density on the nitrogen in position 9, did not display remarkable effects on the inhibitory power.

On the other hand, the presence of an heptyl chain on the nitrogen in position 9 triggered a drastic change in the inhibitory pattern and an increase in affinity, confirming the key role of this moiety in modulating the interaction with the enzyme. Our results suggest that the heptyl chain of **1b** may reach the PAS where it undergoes interaction by the terminal methyl group. This hypothesis is supported by a previous study, where Tacrine derivatives bearing in N-9 position an ω-phenyl alkyl chain were examined [48]. In that case a spacing of 6–7 methylene groups between THA and the phenyl ring was associated with the maximal effect on AChE catalytic function. The increased hydrophobicity of these alkyl derivatives joined with an optimized molecular shape leads to a simultaneous interaction with the catalytic and the peripheral anionic sites.

In conclusion, the study of the interactions of the two Tacrine derivatives with AChE from Electrophorus Electricus in solution by NMR techniques allowed the identification of the specific groups of the ligands interacting with the enzyme, and the evaluation of the interaction constant for both compounds.

The aromatic portion of both molecules was the most involved in binding, because the correlation times of protons 7 and 8 resulted to be mostly slowed down in the presence of the enzyme. Compound **1b** displayed a further interaction with the enzyme by its hydrophobic tail, by that showing a higher affinity than **1a**.

Appendix A. Supplementary data

Supplementary data associated with this article can be found, in the online version, at doi:10.1016/j.bioorg.2007.01.001.

References

[1] J. Birks, Cochrane Database Syst. Rev. 25 (2006) CD005593.
[2] A. Takeda, E. Loveman, A. Clegg, et al., Int. J. Geriatr. Psychiatry 21 (2006) 17–28.
[3] L.S. Schneider, I.R. Kats, S. Park, J. Napolitano, R.A. Martinez, S.P. Azen, Am. J. Geriatr. Psychiatry 11 (2003) 414–425.
[4] L.J. Scott, K.L. Goa, Drugs 60 (2000) 1095–1122.
[5] C. Loy, L. Schneider, Cochrane Database Syst. Rev. 25 (2006) CD001747.
[6] P.T. Francis, A. Nordberg, S.E. Arnold, Trends Pharmacol. Sci. 26 (2005) 104–111.
[7] M. Smith, J. Wells, M. Borrie, Alzheimer Dis. Assoc. Disord. 20 (2006) 133–137.
[8] M.L. Bolognesi, V. Andrisano, M. Bartolini, R. Banzi, C. Melchiorre, J. Med. Chem. 48 (1) (2005) 24–27.
[9] A.H. Moore, M.K. O'Banion, Adv. Drug Deliv. Rev. 54 (2002) 1627–1656.
[10] J.T. Rogers, D.K. Lahiri, Curr. Drug Targets 5 (2004) 535–551.
[11] M. Bartolini, C. Bertucci, V. Cavrini, V. Andrisano, Biochem. Pharmacol. 65 (2003) 407–416.
[12] A. Nunomura, R.J. Castellani, X. Zhu, P.I. Moreira, G. Perry, M.A. Smith, J. Neuropathol. Exp. Neurol. 65 (2006) 631–641.
[13] A. Akaike, Alzheimer Dis. Assoc. Disord. 20 (2006) S8–S11.
[14] G. Amitai, R. Adani, E. Fishbein, H. Meshulam, I. Laish, S. Dachir, Chem. Biol. Interact. 157–158 (2005) 361–363.
[15] D. Alonso, I. Dorronsoro, L. Rubio, P. Munoz, E. Garcia-Palomero, M. Del Monte, A. Bidon-Chanal, M. Orozco, F.J. Luque, A. Castro, M. Medina, A. Martinez, Bioorg. Med. Chem. 13 (2005) 6588–6597.
[16] M.I. Rodriguez-Franco, M.I. Fernandez-Bachiller, C. Perez, B. Hernandez-Ledesma, B. Bartolome, J. Med. Chem. 49 (2006) 459–462.
[17] M. Rosini, V. Andrisano, M. Bartolini, M.L. Bolognesi, P. Hrelia, A. Minarini, A. Tarozzi, C. Melchiorre, J. Med. Chem. 48 (2005) 360–363.
[18] P. Camps, R. El Achab, D.M. Görbig, J. Morral, D. Muñoz-Torrero, A. Badia, J.E. Bañoz, N.M. Vivas, X. Barril, M. Orozco, F.J. Luque, J. Med. Chem. 42 (1999) 3227–3242.
[19] M.R. Del Giudice, A. Borioni, C. Mustazza, F. Gatta, A. Meneguz, M.T. Volpe, Il Farmaco 51 (1996) 693–698.
[20] L. Fielding, Tetrahedron 56 (2000) 6151–6170.
[21] E. Cernia, M. Delfini, M.E. Di Cocco, C. Palocci, S. Soro, Bioorg. Chem. 30 (2002) 276–284.
[22] M. Delfini, C. Bianchetti, M.E. Di Cocco, N. Pescosolido, F. Porcelli, R. Rosa, G. Rugo, Bioorg. Chem. 31 (2003) 378–388.
[23] M. Delfini, R. Gianferri, V. Dubbini, C. Manetti, E. Gaggelli, G. Valensin, J. Magn. Reson. 144 (2000) 129–133.
[24] A. Massiah, C. Viragh, P.M. Reddy, I.M. Kovach, J. Johnson, T.L. Rosenberry, A.S. Mildvan, Biochemistry 40 (2001) 5682–5690.
[25] Y. Li, Q. Li, M. Sun, G. Song, S. Jiang, D. Zhu, Bioorg. Med. Chem. Lett. 14 (2004) 1585–1588.
[26] I. Correia, N. Ronzani, N. Platzer, B.T. Doan, J.C. Beloeil, J. Phys. Org. Chem. 19 (2006) 148–156.
[27] L. Sussman, M. Harel, F. Frolow, C. Oefner, A. Goldman, L. Toker, I. Silman, Science 253 (1991) 872–879.
[28] C.E. Felder, M. Harel, I. Silman, J.L. Sussman, Acta Crystallogr. D 58 (2002) 1765–1771.
[29] J.P. Colletier, D. Fournier, H.M. Greenblatt, J. Stojan, J.L. Sussman, G. Zaccai, I. Silman, M. Weik, EMBO J. 25 (2006) 2746–2756.

[30] Y. Bourne, Z. Radić, H.C. Kolb, K.B. Sharpless, P. Taylor, P. Marchot, Chem. Biol. Interact. 157–158 (2005) 159–165.
[31] C.H.T.P. da Silva, V.L. Campo, I. Carvalho, C.A. Taft, J. Mol. Graph. Model. 25 (2006) 169–175.
[32] H. Dvir, D.M. Wong, M. Harel, X. Barril, M. Orozco, F.J. Luque, D. Muñoz-Torrero, P. Camps, T.L. Rosenberry, I. Silman, J.L. Sussman, Biochemistry 41 (2002) 2970–2981.
[33] M.M. Hurley, A. Balboa, G.H. Lushington, J. Guo, Chem. Biol. Interact. 157-158 (2005) 321–325.
[34] F. Porcelli, M. Delfini, M.R. Del Giudice, Bioorg. Chem. 27 (1999) 197–205.
[35] R. Freeman, H.D.W. Hill, B.L. Tomlinson, L.D. Hall, J. Chem. Phys. 61 (1974) 4466–4473.
[36] L.D. Hall, H.D.W. Hill, J. Am. Chem. Soc. 98 (1976) 1269–1270.
[37] G. Valensin, T. Kushnir, G. Navon, J. Magn. Reson. 46 (1982) 23–29.
[38] M.E. Amato, K.B. Lipkowitz, G.M. Lombardo, G.C. Pappalardo, J. Chem. Soc. Perkin. Trans. 2 (1995) 321.
[39] R. Faure, G. Giovannangeli, J.P. Galy, J.C. Soyfer, E.J. Vincent, J. Barbe, Journal de Chimie Physique 78 (1981) 527–530.
[40] E. Gaggelli, G. Valensin, T. Kushnir, G. Navon, Magn. Reson. Chem. 30 (1992) 461–465.
[41] T. Sai, N. Takao, M. Sugiura, Magn. Reson. Chem. 30 (1992) 1041–1046.
[42] M.R. Del Giudice, M. Delfini, N. Travaglini, Quart. Magn. Res. Biol. Med. III (2) (1996) 93–97.
[43] P. Muñoz-Ruiz, L. Rubio, E. Garcìa-Palomero, I. Dorronsoro, M. del Monte-Millán, R. Valenzuela, P. Usán, C. de Austria, M. Bartolini, V. Andrisano, A. Bidon-Chanal, M. Orozco, F.J. Luque, M. Medina, A. Martínez, J. Med. Chem. 48 (2005) 7223–7233.
[44] G. Veglia, M. Delfini, M.R. Del Giudice, E. Gaggelli, G. Valensin, J. Magn. Reson. 130 (1998) 281–286.
[45] E. Gaggelli, G. Valensin, Concepts Magn. Reson. 5 (1993) 19–42.
[46] X. Barril, M. Orozco, F.J. Luque, J. Med. Chem. 42 (1999) 5110–5119.
[47] D. Han, P. Yang, J. Mol. Struct. (Theochem) 668 (2004) 25–28.
[48] Y.P. Pang, P. Quiram, T. Jelacic, F. Hong, S. Brimijoin, J. Biol. Chem. 271 (1996) 23646–23649.